Experimental Measurement of Angular Anisoplanatism for Sodium Laser Guide Star: Synchronized Range Gating Realization

Xi Luo, Xinyang Li, Xiaoyun Wang and Kui Huang
The Laboratory on Adaptive Optics, Institute of Optics and Electronics, Chinese Academy of Sciences, P. O. Box 350, Shuangliu, Chengdu, Sichuan 610209, China
The Key Laboratory on Adaptive Optics, Chinese Academy of Sciences, P. O. Box 350, Shuangliu, Chengdu, Sichuan 610209, China

Keywords: Adaptive Optics, Sodium Laser Guide Star, Angular Anisoplanatism, Range Gating Mechanism, Synchronized Timing Control, Experimental Measurement.

Abstract: Laser Guide Star (LGS) is an ideal synthetic beacon of Adaptive Optics (AO) for compensating for the atmospheric turbulence induced wave-front distortion of the science object; however the unavoidable anisoplanatism resulting from different light experience between the LGS and the science object through turbulent atmosphere will lead to a degradation of compensation performance, especially for the angular anisoplanatism in sodium LGS AO. By using our developed Hartmann-Shack (HS) wave-front sensor with accurate range gating mechanism, the return-light spot arrays through turbulent atmosphere from the natural star and the excited sodium LGS with certain angular offsets can be synchronously collected. Different from our previously published work (Luo *et al*., 2018), the experimental set-up, the structural design of the range gating mechanism, and the timing design of the synchronized control are discussed emphatically in this paper. The typical experimental measurement result of the angular anisoplanatism for the sodium LGS with 10” angular offsets is just briefly presented, which is basically consistent with our previous numerical simulation result (Luo *et al*., 2015). The majority of Zernike-modal de-correlations between the sodium LGS and the science object occur obviously, as the sodium LGS reference moving outside of the optical path from the science object to the telescope aperture.

1 INTRODUCTION

Adaptive Optics (AO) applied for compensating for turbulent atmosphere in real time usually requires a sufficiently bright reference source in the isoplanatic patch around the science object to provide a desired measurement of the wave-front distortion induced from atmospheric turbulence. The concept of Laser Guide Star (LGS) has been publicly proposed to overcome the limitations due to finite sky-coverage (Foy and Labeyrie, 1985), which is generated by illuminating a ground-based laser in the specific atmosphere layer to provide the backscattered light with information on the wave-front distortion introduced by atmospheric turbulence, including the Rayleigh LGS (Fugate *et al*., 1991) and the sodium LGS (Humphreys *et al*., 1991). Profiting from its higher altitude with better sampling of atmospheric turbulence, the sodium LGS has been received worldwide attention since its concept was first put forward (Fugate *et al*., 1994; Bonaccini, Hackenberg, and Avila, 1998; Joyce, *et al*., 2006). Anisoplanatism results from different turbulence experience along the optical path by light from the LGS and the science object, which is one of the fundamental limitations to preventing an ideal LGS AO performance. Since atmospheric turbulence strength is distributed and varied with altitude in front of the aperture of receiving telescope, comparing with focal anisoplanatism just induced from the finite altitude for the LGS reference coinciding with the science object, angular separation (namely, angular anisoplanatism) results in two lights traversing different regions in atmospheric turbulence, and arises an deterioration of the partial Zernike-modal correlations between the LGS reference and the science object, especially for the sodium LGS with greater angular separation.

As the theoretical investigation has progressed (Molodij and Rousset, 1997; Sasiela, 2007), with the rapid development of the sodium LGS technology

Luo, X., Li, X., Wang, X. and Huang, K.
Experimental Measurement of Angular Anisoplanatism for Sodium Laser Guide Star: Synchronized Range Gating Realization.
DOI: 10.5220/0007308401020109
In *Proceedings of the 7th International Conference on Photonics, Optics and Laser Technology (PHOTOPTICS 2019)*, pages 102-109
ISBN: 978-989-758-364-3

and its application in engineering, also the experimental investigations on the sodium LGS anisoplanatism have been carried out. For example, the experimental measurement of anisoplanatic degradation of K-band Strehl ratio on the 10-m Keck II telescope (Van Dam *et al.*, 2006), the experimental measurement of focal anisoplanatism carried out by China Academy of Engineering Physics (Chen *et al.*, 2015), etc.. However, to the best of our knowledgement, there has been no public report on the quantitative measurements of angular anisoplanatic error for the sodium LGS in literature. By using our developed HS wave-front sensor with accurate range gating actualization, the synchronized experimental measurement of angular anisoplanatic effect for the sodium LGS can be achieved.

The emphasises of this paper are on the discussions of the experimental set-up, the structural design of the range gating mechanism, and the timing design of the synchronized control. In order to maintain the integrity of this paper, the typical experimental results of the wave-front distortion decomposed Zernike-modal correlations between the natural star and the sodium LGS reference with 10" angular offsets, and the angular anisoplanatism decomposed Zernike-modal relative errors for the off-axis sodium LGS reference are just briefly presented. For the detailed disscusion of the achieved angular anisoplanatism experimental data, readers could find answer in our previously published work (Luo *et al.*, 2018).

2 EXPERIMENTAL SET-UP

The experimental set-up of synchronized angular anisoplanatism measurement for sodium LGS is outlined in Figure 1, which includes the telescope with clear aperture of 1m, the pulsed sodium LGS laser source with wavelength centered on the mesospheric sodium D_2 line, the Tilt Mirror (TM) for pointing control of the sodium LGS laser source projection to sky, the synchronized control module, the developed HS wave-front sensor with accurate range gating mechanism, and the corresponding processor for the wave-front recovery and the TM actuation.

As shown in Figure 1, in the experiment, the telescope works in closed-loop to track an appropriate natural star in the sky with azimuth angle A and elevation angle E, and the incident laser beam of the sodium LGS laser source is reflected off the TM and projected to the mesospheric layer for generating the resonant backscattered sodium LGS with its angular distance θ from the natural star closed-loop controlled by the TM. On the basis of the synchronized control reference signal provided from the HS wave-front sensor, in every laser shot, the temporal synchronization of the laser source emission and the resulting resonant backscattered sodium LGS detection with the HS wave-front sensor can be achieved via the synchronized control module. Consequently, two sets of the synchronous wave-front distortion sequences can be recovered with the return-light spot arrays through turbulent atmosphere from the on-axis natural star and the off-axis sodium LGS. Furthermore, the anisoplanatic error's Zernike-modal statistics for the off-axis sodium LGS can be derived from the two sets of the recovered wave-front distortion sequences.

2.1 HS Wave-front Sensor with Accurate Range Gating Actualization

The schematic diagram of the HS wave-front sensor is illustrated in Figure 2, along the direction of the return-light propagation, which consists of the beam compressing optical system with compression ratio of 6:1, the mechanical shutter device, the microlens array, the matched imaging optical system with magnification of 2:1, and the Charge Coupled Device (CCD) camera. The corresponding field of view of each sub-aperture is 21.9".

In our developed HS wave-front sensor, the adoption of mechanical shutter technology is an effective way to selecting the resonant backscatter from the sodium atoms in the mesospheric layer (at the altitude of approximately 80~100km), and meanwhile to obstructing the Rayleigh backscatter from the air molecules in the short-range atmosphere (at the altitude of approximately below 30km).

As shown in Figure 2 and Figure 3, the mechanical shutter device includes the photoelectric switch sensor, the rotary optical-chopping disc and its motor driven. The rotary optical-chopping disc is vertically mounted at the optical focus of entry lens of the beam compressing optical system. For the repetitively pulsed sodium resonant backscattered light unobstructed propagation and collection, there are a number of slots with central angle φ are rotational-symmetrically manufactured on the edge of the optical-chopping disc. In practice, the number of the slots M depends on the output pulse repetition frequency of the sodium LGS laser source f and an appropriate rotational speed of the optical-chopping disc N (namely, M×N=f). At the same time, the output pulse-width of the sodium LGS laser source

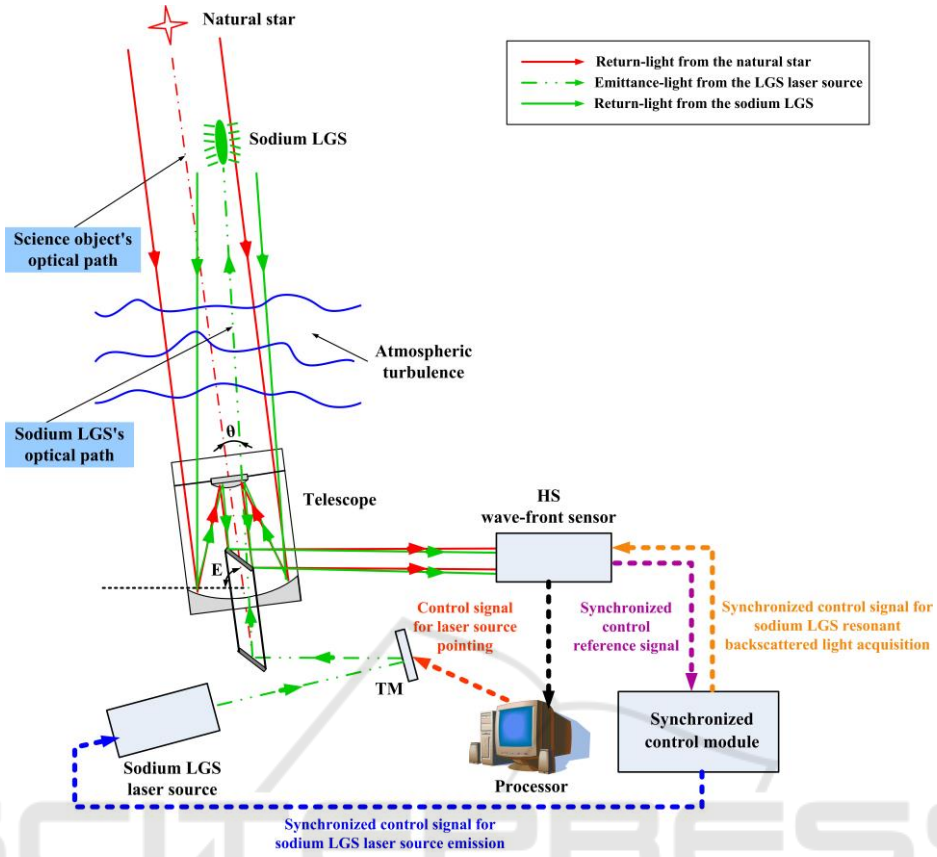

Figure 1: The experimental set-up of synchronized angular anisoplanatism measurement for sodium LGS.

Δt_{Pulse}, the sampled thickness of the sodium layer ΔH, the accommodation to the elevation angle E variation for the sodium LGS observation, and the transition time from the open-started state to the open-completed state of the receiving optical path of the HS wave-front sensor Δt_{rising} must be taken into account in the design of the central angle φ of every single slot on the optical-chopping disc (namely, $\varphi \geq (2\times\Delta H/\sin E/c+\Delta t_{pulse}+\Delta t_{rising}) \times N\times 360$).

As the optical-chopping disc stably rotates, the receiving optical path on-off state of the HS wave-front sensor is periodically modulated, and the synchronized control reference signal of the same frequency as the sodium LGS laser source emission is obtained from the photoelectric switch sensor reading the slots on the disc, whose duty cycle equals to $(\varphi\times f)/(N\times 360)$. Based on this synchronized control reference signal, the sodium LGS laser

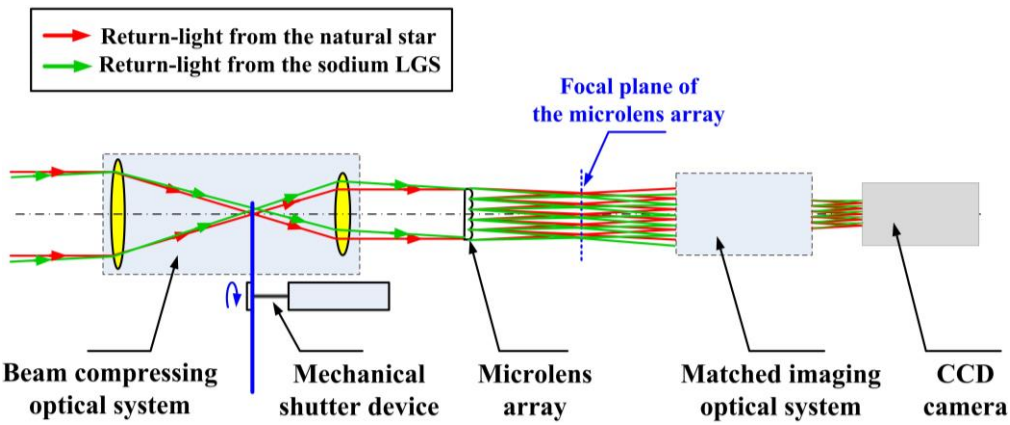

Figure 2: The schematic diagram of the HS wave-front sensor with range gating mechanism.

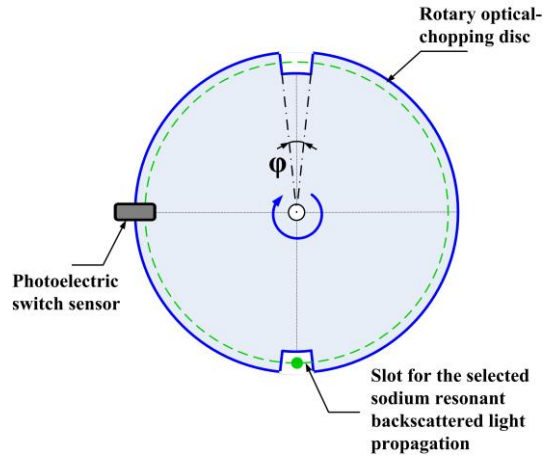

Figure 3: The schematic diagram of the mechanical shutter device.

source emission and the resulting resonant backscattered sodium LGS detection with the CCD camera can be temporally synchronized. Within every launch period of the sodium LGS laser source, it is synchronously confirmed that the receiving optical path is not in completely on state until the resonant backscattered light resulting from the interaction between the emitted laser pulse and the mesospheric sodium atoms arrives at the aperture of the telescope.

2.2 Synchronized Control Process for Sodium LGS Laser Source Emission and Its Resulting Resonant Backscattered Light Collection

In order to select the resonant backscatter from the sodium atoms in the mesospheric layer and to obstruct the Rayleigh backscatter from the air molecules in the short-range atmosphere by effectively range gating, the synchronized control process for the pulsed sodium LGS laser source emission and its resulting resonant backscattered light collection is designed.

In Figure 4 the synchronized control process for the pulsed sodium LGS laser source emission and its resulting resonant backscattered light collection is outlined:

(1) $\Delta t_{on}=\varphi/(N\times 360)$ is the high level duration of the synchronized control reference signal obtained from the photoelectric switch sensor; $\Delta t_1=2\times H_{begin}\times cscE/c$ is the arrive time of the resonant backscattered light from the bottom of the sodium layer at the altitude of H_{begin} after each laser pulse emitting; $\Delta t_{sodium\text{-}LGS}=2\times\Delta H\times cscE/c+\Delta t_{pulse}$ is the temporal duration of the resonant backscattered light resulting from the interaction between the sodium atoms in the mesospheric layer and the emitted laser pulse with pulse-width of Δt_{pulse}.

(2) Δt_{rising} is the transition time from the open-started state to the open-completed state of the receiving optical path of the HS wave-front sensor; Δt_0 is the time delay between the rising edge of the synchronized control reference signal and the open-completed state of the receiving optical path of the HS wave-front sensor; both of them can be accurately measured in advance by high-speed photodetector and oscilloscope.

(3) $\Delta t_{laser\text{-}delay}=\Delta t_0-\Delta t_1$ is the time delay between the rising edge of the synchronized control reference signal and the rising edge of the synchronized control signal for the pulsed sodium LGS laser source emission; $\Delta t_{CCD\text{-}delay}=\Delta t_0$ is the time delay between the rising edge of the synchronized control reference signal and the rising edge of the synchronized control signal for the sodium LGS resonant backscattered light exposure by the CCD camera.

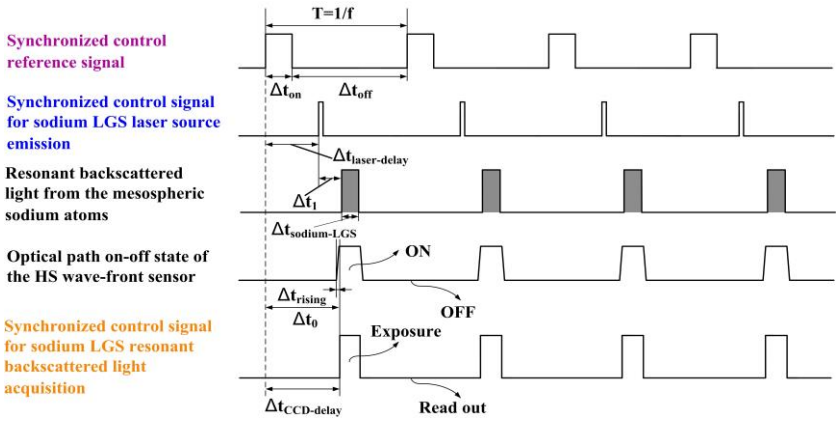

Figure 4: The designed timing diagram of the sodium LGS resonant backscattered light synchronized collection.

3 POST-PROCESSING OF EXPERIMENTAL DATA

Based on the experimental set-up (as shown in Figure 1), the structural design of the mechanical shutter device (as shown in Figure 3), and the timing design of the sodium LGS synchronized collection (as shown in Figure 4), as time goes by, the sequences of the return-light spot arrays through turbulent atmosphere from the natural star and the sodium LGS with certain angular offsets can be synchronously collected by the HS wave-front sensor.

Afterwards, from the mutiple-frame sequences of the return-light spot arrays collected by the HS wave-front sensor, the synchronous turbulence-induced wave-front distortion sequences can be recovered for the on-axis natural star and the off-axis sodium LGS, respectively:

$$\varphi_{STAR}(Rr,\vartheta)=\sum_{j=3}^{K} a_{j-STAR}\times Z_j(r,\vartheta)$$
$$\varphi_{LGS}(Rr,\vartheta,\theta)=\sum_{j=4}^{K} a_{j-LGS}\times Z_j(r,\vartheta) \quad (1)$$

where R is the clear aperture radium of the telescope, $Z_j(r,\vartheta)$ is the j th-order Zernike polynomial (Noll, 1976), $a_{j\text{-}STAR}$ is the decomposed j th-order Zernike-modal coefficient of the wave-front distortion of the on-axis natural star, $a_{j\text{-}LGS}$ is the decomposed j th-order Zernike-modal coefficient of the wave-front distortion of the off-axis sodium LGS, and K is the corresponding highest-order Zernike mode of the recovered wave-front distortion by the HS wave-front sensor (e.g. K=35). The total-tilt terms (e.g. j=1, 2) for the on-axis natural star, and the total-tilt and defocus terms (e.g. j=1, 2, 3) for the off-axis sodium LGS are not included in the recovered wave-front distortion.

Consequently, the recovered wave-front distortion decomposed Zernike-modal correlations between the on-axis natural star and the off-axis sodium LGS, and the angular anisoplanatism decomposed Zernike-modal relative errors for the off-axis sodium LGS can be calculated by the equation (2) and equation (3), respectively:

$$r_j=\frac{COV\left(a_{j-STAR},a_{j-LGS}\right)}{\sqrt{\left\langle a^2_{j-STAR}\right\rangle}\times\sqrt{\left\langle a^2_{j-LGS}\right\rangle}} \quad (j\geq 4) \quad (2)$$

$$\varepsilon_j^2=\frac{\left\langle\left(a_{j-STAR}-a_{j-LGS}\right)^2\right\rangle}{\left\langle a^2_{j-STAR}\right\rangle} \quad (j\geq 4) \quad (3)$$

where COV denotes the covariance, and < > denotes the ensemble average.

4 TYPICAL EXPERIMENTAL RESULTS

In this section, for the integrity of this paper, we just briefly present the typical experimental result of angular anisoplanatism measurement for the sodium LGS with 10” angular offsets, which has been partially published in our previous work (Luo *et al*., 2018).

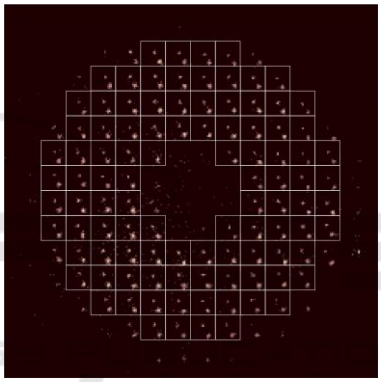

Figure 5: The typical single frame of the return-light spots arrays from the natural star and the sodium LGS with 10” angular offsets (Luo *et al*., 2018).

H_{begin} is chosen to be 75km for timing rejection of the Rayleigh back scattering. The typical single frame of the return-light spot arrays through turbulent atmosphere from the natural star with azimuth angle A of 70º and elevation angle E of 75º and the sodium LGS with 10” angular offsets is shown in Figure 5 (Luo et al., 2018), the whole return-light spot arrays from the natural star are located at the center of the sub-apertures, and the whole return-light spot arrays from the sodium LGS with 10” angular offsets are located at the bottom right of the sub-apertures.

The first 20th Zernike-modal correlations of the recovered wave-front distortion between the on-axis natural star and the off-axis sodium LGS with 10” angular offsets are calculated and shown in Figure 6. Good correlations only exist in the low-order Zernike modes of the two types of wave-front distortions from the on-axis natural star and the off-

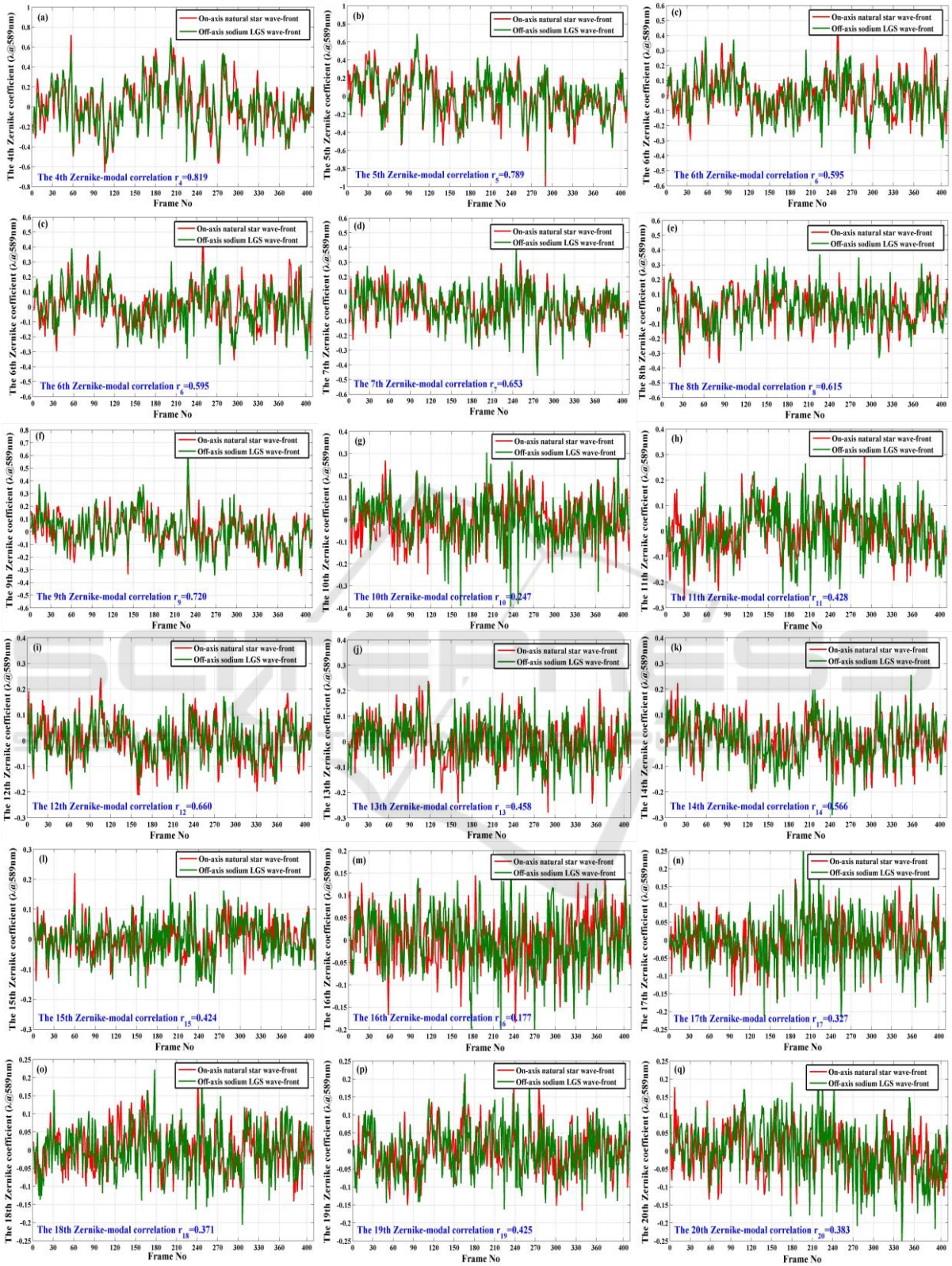

Figure 6: The typical experimental result of the first 20th Zernike-modal correlations of the recovered wave-front distortion between the on-axis natural star and the off-axis sodium LGS with 10” angular offsets.

axis sodium LGS, respectively (e.g., the average of the Zernike-modal correlation $<r_j>$=0.70 for j=4~9). Increasing the Zernike-modal order j means deteriorating correlation r_j, the average of the Zernike-modal correlation $<r_j>$=0.46 for j=10~15, but the average of the Zernike-modal correlation $<r_j>$=0.33 for j=16~20.

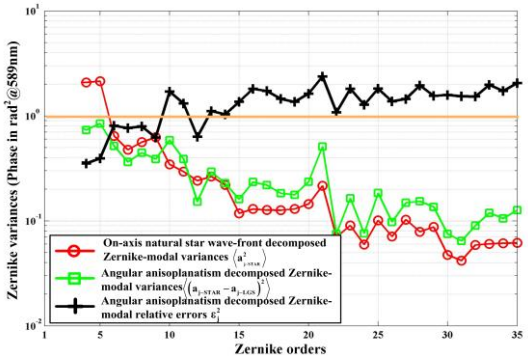

Figure 7: The typical experimental result of the angular anisoplanatism decomposed Zernike-modal relative errors for the off-axis sodium LGS with 10" angular offsets (Luo *et al*., 2018).

The corresponding angular anisoplanatism decomposed Zernike-modal relative errors for the off-axis sodium LGS are calculated and illustrated in Figure 7 (Luo *et al*., 2018). Resulting from improper turbulent atmosphere probing with the off-axis sodium LGS as reference on the outside of the optical path from the natural star to the telescope aperture, obvious de-correlations occur between the majority of Zernike modes of the two types of wave-front distortions from the on-axis natural star and the off-axis sodium LGS, and the corresponding angular anisoplanatism decomposed Zernike-modal relative errors are bigger than one. This phenomenon is basically consistent with our previous numerical simulation work (Luo *et al*., 2015).

5 CONCLUSIONS

By means of the structural design of the range gating mechanism accompanied with the synchronized timing design of the sodium LGS excitation and collection, the synchronized return-light spot arrays through turbulent atmosphere from the science object and the excited sodium LGS with certain angular offsets can be collected by using our developed HS wave-front sensor, which provides a convenient way to experimental measurement of the angular anisoplanatism for LGS. Further investigation in this area will be carried out in the future.

ACKNOWLEDGEMENTS

This work has been supported by the Young Scientists Fund of the National Natural Science Foundation of China (Grant No. 61505215).

REFERENCES

Luo, X., Li, X.Y., Hu, S.J., Huang, K., Wang, X.Y., 2018, Experimental investigation of angular anisoplanatism for sodium beacon. *Acta Physica Sinica*, 67 (9), 099501. (In Chinese)

Luo, X., Li, X.Y., Shao, L., Hu, S.J., Huang, K., 2015. Investigation of anisoplanatic effect in adaptive optics for atmospheric turbulence correction. In *Proceedings of SPIE, the 20th International Symposium on High-Power Laser Systems and Applications*. SPIE Press.

Foy, R., Labeyrie, A., 1985, Feasibility of adaptive telescope with laser probe. *Astronomy and Astrophysics*, 152 (2), L29-L31.

Fugate, R.Q., Fried, D.L., Ameer, G.A., Boeke, B.R., Browne, S.L., Roberts, P.H., Ruane, R.E., Tyler, G.A., Wopat, L.M., 1991, Measurement of atmospheric wavefront distortion using scattered light from a laser guide star. *Nature*, 353 (6340), 144-146.

Humphreys, R.A., Primmerman, C.A., Bradley, L.C., Herrmann, J., 1991, Atmospheric-turbulence measurements using synthetic beacon in the mesospheric sodium layer. *Optics Letters*, 16 (18), 1367-1369.

Fugate, R.Q., Ellerbroek, B.L., Higgins, C.H., Jelonek, M. K., Lange, W.J., Slavin, A.C., Wild, W.J., Winker, D.M., Wynia, J.M., Spinhirne, J.M., Boeke, B.R., Ruane, R.E., Moroney, J.F., Oliker, M.D., Swindle, D.W., Cleis, R.A., 1994, Two generations of laser-guide-star adaptive-optics experiments at the Starfire Optical Range. *Journal of the Optical Society of America A*, 11 (1), 310-324.

Bonaccini, D., Hackenberg, W., Avila, G., 1998. Laser guide star facility for the ESO VLT. In *Proceedings of SPIE, Adaptive Optical System Technologies*. SPIE Press.

Joyce, R., Boyer, C., Daggert, L., Ellerbroek, B., Hileman, E., Hunten, M., Liang, M., 2006. The laser guide star facility for the Thirty Meter Telescope. In *Proceedings of SPIE, Advances in Adaptive Optics II*. SPIE Press.

Molodij, G., Rousset, G., 1997, Angular correlation of Zernike polynomials for a laser guide star in adaptive optics. *Journal of the Optical Society of America A*, 14 (8), 1949-1966.

Sasiela, R.J., 2007. *Electromagnetic wave propagation in turbulence: evaluation and application of Mellin transforms*, SPIE Press. Washington, 2nd edition.

Van Dam, M.A., Sasiela, R.J., Bouchez, A.H., Mignant, D.L., Campbell, R.D., Chin, J.C.Y., Hartman, S.K., Johansson, E.M., Lafon, R.E., Stomski, P.J., Summers, D.M., Wizinowich, P.L., 2006. Angular anisoplanatism in laser guide star adaptive optics. In *Proceedings of SPIE, Advances in Adaptive Optics II*. SPIE Press.

Chen, T.J., Zhou, W.C., Wang, F., Huang, D.Q., Lu, Y.H., Zhang, J.Z., 2015, Experimental research on focusing anisoplanatism of sodium guide star via synchronous pulse detection. *Acta Physica Sinica*, 64 (13), 134207. (In Chinese)

Noll, R.J., 1976, Zernike polynomials and atmospheric turbulence. *Journal of the Optical Society of America*, 66 (3), 207-211.